Zeitschrift: Eclogae Geologicae Helvetiae
Herausgeber: Schweizerische Geologische Gesellschaft
Band: 97 (2004)
Heft: 1

Artikel: Alpine and late-hercynian geochronological constraints in the Argentera Massif (Western Alps)
Autor: Corsini, Michel / Ruffet, Gilles / Caby, Renaud
DOI: https://doi.org/10.5169/seals-169093

0012-9402/04/010003-13
DOI 10.1007/s00015-004-1107-8
Birkhäuser Verlag, Basel, 2004

Eclogae geol. Helv. 97 (2004) 3–15

Alpine and late-hercynian geochronological constraints in the Argentera Massif (Western Alps)

MICHEL CORSINI[1], GILLES RUFFET[2] & RENAUD CABY[3]

Key words: ^{39}Ar-^{40}Ar geochronology, Western Alps, Argentera, Alps, Hercynian

ABSTRACT

Located in the southern part of the Western Alps, the Argentera massif belongs to the paleo-European basement of the external domain. It experienced a polyphased deformation history, Hercynian and Alpine. The Alpine history is characterized by the development of a network of ductile shear zones. An ^{39}Ar-^{40}Ar study of single grains of Hercynian muscovites and Alpine phengites allowed to constrain various events. A muscovite cooling age at ca 296-299 Ma is proposed for the Argentera granite, clearly later than the estimated cooling age at ca 310-315Ma for the low-pressure anatexis. Neocrystallized phengites collected within an Alpine shear zone (Frema Morte) crosscutting the late Hercynian Argentera granite yielded an age at 22.2 ± 0.3 Ma (1σ). This is one of the first unequivocal absolute age constraint of a late Alpine metamorphism in the external crystalline massifs of the Western Alps. Our P-T conditions estimates indicate a regional temperature at ca 350 °C for pressure at 0.35-0.4 GPa for this Alpine metamorphism. These estimates imply a minimum burial of 14 km for the Argentera massif, which could result from the overloading imposed by the internal nappes emplacement, probably between 28 Ma and 22.2 Ma.

RESUME

Le massif de l'Argentera est le massif cristallin externe le plus méridional externe de la chaîne alpine. Rattaché au socle européen, ce massif est marqué par une histoire polyphasée, hercynienne et alpine. La déformation alpine se concentre essentiellement dans un réseau de zones de cisaillements ductiles. Une étude ^{39}Ar-^{40}Ar sur monograins de muscovites hercyniennes et de phengites alpines permet de mieux comprendre l'évolution du massif. Un âge à environ 296-299 Ma obtenu sur les muscovites du granite de l'Argentera montre que sa mise en place est postérieure à l'épisode d'anatexie crustale tardi-collisionnelle qui se manifeste à environ 310-315Ma. L'analyse des phengites néoformées provenant de la zone de cisaillement alpine de Frema Morte qui recoupe le granite hercynien de l'Argentera a fourni un age à 22.2 ± 0.3 Ma (1σ). Ce résultat permet de contraindre l'âge du métamorphisme alpin qui affecte tardivement les massifs cristallins externes dans les Alpes occidentales. Notre étude sur les conditions du métamorphisme alpin suggère d'autre part une température régionale d'environ 350 °C pour une pression de 0.35-0.4 GPa. Ces estimations impliquent un enfouissement minimum du massif de l'Argentera d'environ 14 km, en relation avec les nappes internes qui se mettent en place probablement entre 28 Ma et 22.2 Ma.

1. Introduction

The External Crystalline Massifs (Aar – Gotthard, Mont Blanc – Aiguilles Rouges, Belledone, Pelvoux and Argentera) outcrop along the external domain of the Western Alps (Fig.1). These basement units belong to the polymetamorphic European crust which was affected during the Alpine collisional shortening by crustal scale thrust with a few kilometers displacement below the external massifs (Mugnier et al.1990). Located in the southern part of the Western Alps, the Argentera crystalline massif is mainly composed by migmatitic paragneisses, amphibolites, diatexites and anatectic granitoids, all crosscut by the post metamorphic Argentera granite. These rocks experienced a polyphased deformation history in the context of a high grade Hercynian metamorphism as the other external crystalline massifs (e.g.Von Raumer & Neubauer 1993; Bogdanoff et al.1991).

The present structure of the Argentera massif results from the superposition of Hercynian and Alpine deformation histories. The Alpine history of this massif is classically viewed as limited to the development of ductile shear zones which frequently rework shear zones considered as late-Hercynian (Faure-Muret 1955; Vernet 1964; Malaroda et al. 1970; Bogdanoff 1980). The precise extent and location of Alpine deformation structures are still poorly known and only a few

[1] Géosciences Azur, UMR 6526, Université de Nice – Sophia Antipolis, Parc Valrose, Nice, France. E-mail: corsini@unice.fr
[2] Géosciences Rennes, UMR 6118, Université de Rennes 1, Campus de Beaulieu, 35042 Rennes Cedex, France
[3] Laboratoire de Tectonophysique, Université de Montpellier 2, Montpellier, France

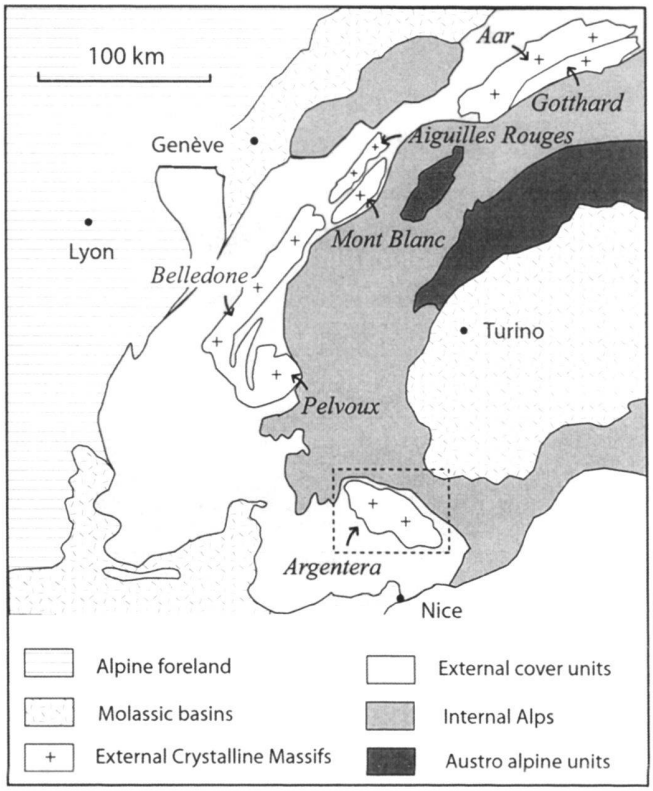

Fig. 1. Location of the External Crystalline Massifs of Western Alps. Studied area localized.

geochronological studies were performed on rocks from this massif (Ferrara & Malaroda 1969; Monié & Maluski 1983; Paquette et al. 1989; Bigot-Cormier et al. 2000; Bogdanoff et al. 2000; Rubatto et al. 2001). The timing of the Alpine deformation is especially poorly constrained (Monié & Maluski 1983; Bigot-Cormier et al. 2000; Bogdanoff et al. 2000).

The aim of this study is to clarify with a powerful geochronological tool, a ^{39}Ar-^{40}Ar laser probe for analyses of single grains of metamorphic and igneous minerals (i) the timing of the late Hercynian thermal evolution, (ii) the precise age of the Argentera granite and (iii) mainly the age of a major Alpine shear zone which crosscuts this granite and the Argentera Massif. The ^{39}Ar-^{40}Ar method is a powerful method to date the deformation. The choice of samples is critical and the analysis of newly crystallized micas from mylonites from the shear zone crosscutting the Argentera granite assures that there is no inheritance of a previous Hercynian deformation event.

2. Pre-Triassic evolution

Two main complexes were identified in the Argentera Massif by Faure-Muret (1955). A NW-SE hectometric mylonitic corridor, the Valetta Shear Zone (Fig.2), separates the occidental complex (Tinée complex) to the west from the oriental complex (Malinvern complex) to the east. The western Tinée complex is constituted of gneisses interlayered with amphibolites, marbles, quartzites, some horizons of graphite schist and a metadiorite. The eastern Malinvern complex is mainly composed of migmatitic gneisses, which are intruded by the late calc-alkaline Argentera granite. Both complexes experienced early eclogitic and granulite metamorphisms followed by a tangential syn-migmatitic event, late tilting of the nappes stack and horizontal shearing (Latouche & Bogdanoff 1987).

Paquette et al. (1989) proposed the existence in the Argentera Massif of two successive episodes of eclogite-facies metamorphism at ca 424 Ma and 351 Ma. Rubatto et al. (2001) questioned these ages because they were obtained on multigrain fractions on ambiguous samples. The latter authors considered two different cases (i) the existence of a single HP-HT Devonian event in the range 443-332 Ma (ii) two distinct HP-HT events Ordovician (eclogitic event, 459-443 Ma) and Devonian (non eclogitic event). Rubatto et al. (2001) proposed also that amphibolite facies metamorphism and anatexis occurred at 323 ± 12 Ma and assigned an Upper Stephanian/Lower Permian age to the Argentera granite (293 Ma; Ferrara & Malaroda 1969, Monié & Maluski 1983).

Late Carboniferous metasediments are preserved in narrow steep belts located close to several major shear zones (Fig. 2). These include black shales and impure sandstones with vertical bedding planes. These rocks may represent remnants of larger basins similar to those of the other External Crystalline Massifs, where they are dated as Stephanian. Permian rocks are restricted to the southeastern part of the massif and consist of continental red beds.

3. Post-Triassic evolution

Mesozoic rocks have been deposited throughout the massif onto a pediplain developed above the eroded basement, as for the other External Crystalline Massifs. Early Triassic sandstones and silts are frequently attached to the basement and form a thin cover of the massif, whereas the overlying Triassic to Early Cretaceous carbonates are mostly detached above the Late Triassic evaporites (Faure-Muret 1955). Upper Cretaceous conglomerates directly deposited on the eroded basement indicate that the NW part of the massif was significantly uplifted at this time. The total thickness of the eroded cover may have reached ca. 3000 m, as evidenced by the thickness of the cover at the southwestern and eastern periphery of the massif. The late Eocene to early Oligocene Annot turbiditic sandstones were deposited in the foreland basin formed west of the Argentera Massif, as it was also the case in the Pelvoux Massif (Champsaur sandstones). This unit may rest directly on the basement in the northwestern part of the massif. The Helminthoid Flysch of Embrunais-Ubaye nappe, between Pelvoux and Argentera Massifs, and of the Ligure nappe, southeast of Argentera Massif, were emplaced on top of the Annot and Champsaur sandstones above olistoliths (Kerck-

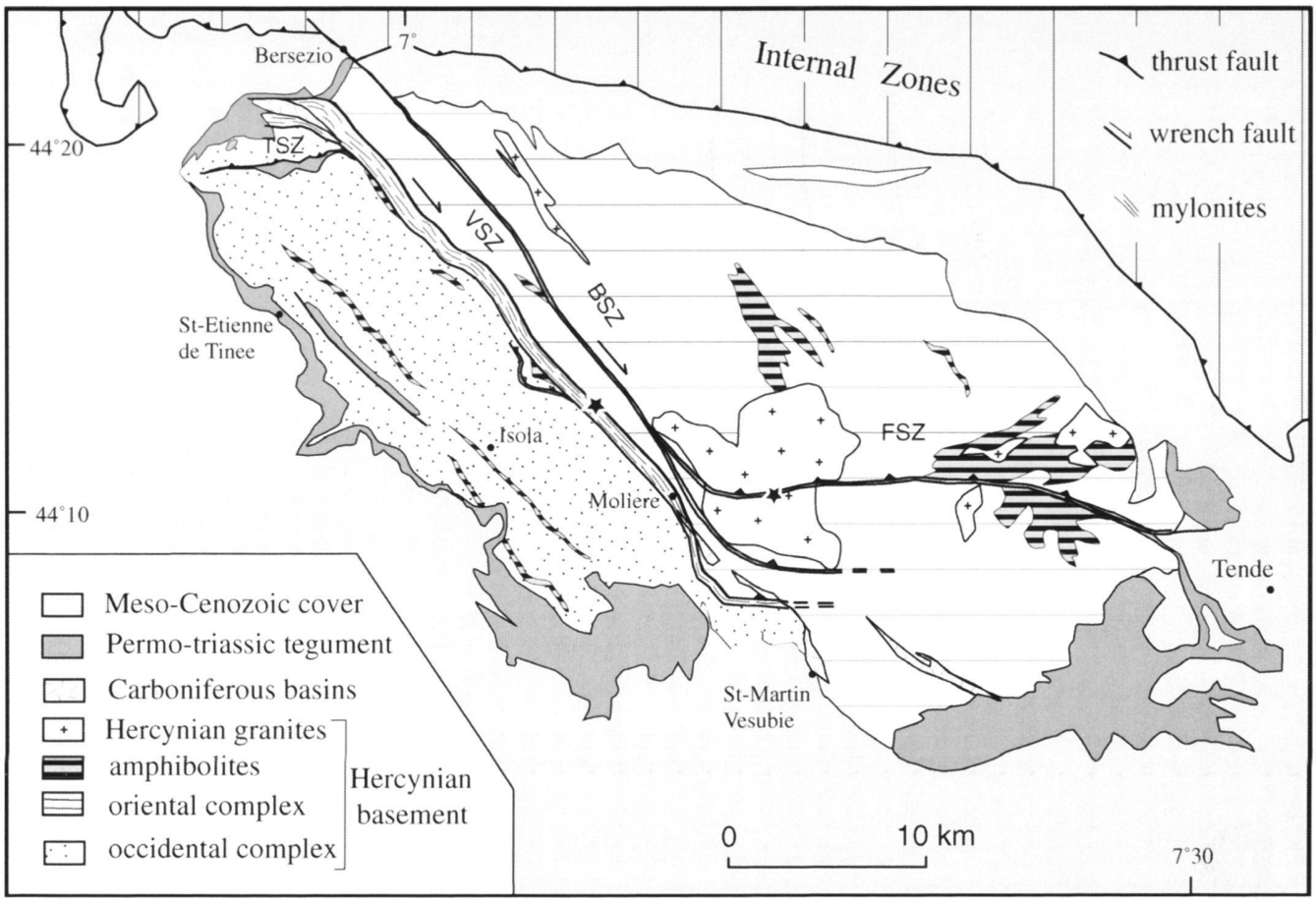

Fig. 2. Schematic geological and structural map of the Argentera massif.
Stars indicate samples locations. VSZ: Valetta shear zone; BSZ: Bersezio shear zone; FSZ: Frema Morte shear zone; TSZ: Tortisse shear zone

hove 1969; Campredon 1977). Southwest of the Argentera Massif, there is evidence that the emplacement of the Helminthoid flysch nappes in the foreland basin occurred after the early Oligocene (at the most 28 Ma), during the Chattian (Ford et al. 1999). This point suggests that the Argentera Massif was deeply buried at this time.

4. Characterization of major alpine structures

Alpine imprint in the Argentera Massif mainly consists in the development of a network of ductile shear zones (Fig. 2). This behaviour is also the main feature of other external crystalline massifs (e.g. the Gotthard, Marquer 1990; the Mont Blanc Gourlay 1986; the Pelvoux, Ford 1996). A great number of shear zones were observed that crosscut the steeply dipping pre-Alpine high-temperature foliation. In the central domain of the massif, between Bersézio to the north and Isola to the south, two main shear zones with a N150-N160 trend can be identified: the Valetta shear zone (VSZ) and the Bersézio shear zone (BSZ). In both shear zones, the steep mylonitic foliation bearing a gently dipping lineation indicates transcurrent movements with a dextral sense of shear evidenced by many shear criteria such as winged porphyroclasts, sigmoidal features and C/S planes. In the southern part of the massif, to the north of Saint Martin de Vésubie, the VSZ splits into several E-W shear zones. The Frema Morte shear zone (FSZ) that is the most important mylonitic corridor among these E-W structures crosscuts the whole eastern part of the massif and the Argentera granite. Along the FSZ the mylonitic foliation progressively dips to the north (30-50°) as it bends, while the lineation keeps consistently a north-south trend. All the shear criteria indicate a reverse sense of shear. In the northwestern part of the Massif, the VSZ splits also into several E-W shear zones (Fig 2). The Tortisse shear zone (TSZ) that is one of these E-W shear zones presents a ca. 50° north dipping with a southward thrusting component.

Upper Carboniferous, Permian and Triassic rocks are involved in these shear zones. It was assumed by our predecessors that the ultramylonites adjacent to Carboniferous rocks might have been formed in connection with Late Carbonifer-

Tab. 1. chemical electron microprobe analyses.
Selected mineral analyses were performed from Cameca Datanim micro-probe Montpellier II University; 20 kV, 10 nA operating conditions; natural silicates as standards, and X-phi data reduction.
- MC6: Phengite 10 from ultramylonite.
- Mer69b: Phengite 35 from a Triassic quartzite.
- Mer72: Phengite 59: phengite from a mylonite in a 2 micas paragneiss
- Mer72:: Biotite 52: Alpine biotite from pressure shadows of pre-Alpine clastic biotites.
- Mer79: Phengite 73: phengite in the matrix of anatectic leucogranite slightly deformed
- Mer79: Phengite 76: phengite from a fissure in a K-feldspar of anatectic leucogranite
- Mer102: Phengite 102 amphibolite
- Mer102: Albite 96: Alpine albite formed at the expense of pre-Alpine plagioclase
- Argo 2: Phengite 136: phengite in an Alpine vein with albite and chlorite
- Argo 2: Chlorite 164: chlorite in an Alpine vein

	MC6	Mer69b	Mer72	Mer79	Mer79	Mer102	Mer72	Mer102	vein	vein
Phe10	Phe35	Phe59	Phe73	Phe76	Phe102	Bi 52	Alb 96	Phe136	Chl 164	
SiO2	47.06	48.79	48.03	47.78	47.50	49.55	45.41	67.13	47.10	24.14
TiO2	0.11	0.39	0.40	0.08	0.01	0.00	0.62	0.00	0.34	0.01
Al2O3	29.64	28.73	28.19	31.43	30.25	29.65	23.62	20.55	27.09	22.11
MgO	1.72	2.34	2.35	1.42	2.19	2.77	3.37	0.01	2.39	17.33
FeO	5.46	4.19	5.02	3.37	3.51	3.15	11.69	0.13	6.20	23.60
MnO	0.06	0.01	0.02	0.03	0.07	0.04	0.11	0.02	0.05	0.13
CaO	0.01	0.02	0.01	0.00	0.01	0.05	0.03	0.70	0.04	0.03
Na2O	0.06	0.04	0.08	0.10	0.12	0.21	1.33	10.85	0.04	0.00
K2O	10.69	11.33	11.23	11.18	11.27	10.84	8.24	0.25	11.23	0.00
H2O	4.38	4.45	4.40	4.45	4.41	4.51	4.22		4.32	11.39
Sum	99.18	100.28	99.72	99.84	99.34	100.76	98.63	99.64	98.81	98.75
Si	3.220	3.288	3.272	3.216	3.224	3.293	3.223	2.948	3.266	2.539
Ti	0.006	0.020	0.020	0.004	0.001	0.000	0.033	0.000	0.018	0.001
Al	2.391	2.281	2.263	2.494	2.420	2.323	1.976	1.064	2.214	2.741
Mg	0.175	0.235	0.239	0.142	0.222	0.275	0.356	0.001	0.247	2.717
Fe2	0.312	0.236	0.286	0.189	0.199	0.175	0.694	0.005	0.360	2.075
Mn	0.003	0.000	0.001	0.001	0.004	0.002	0.007	0.001	0.003	0.011
Ca	0.001	0.001	0.001	0.000	0.001	0.003	0.003	0.033	0.003	0.004
Na	0.009	0.005	0.010	0.013	0.015	0.027	0.182	0.924	0.005	0.000
K	0.933	0.974	0.976	0.960	0.976	0.920	0.746	0.014	0.993	0.001
OH	2.000	2.000	2.000	2.000	2.000	2.000	2.000		2.000	8.000
Sum	9.050	9.041	9.069	9.020	9.061	9.019	9.220	4.989	9.109	18.090

ous basin formation (Faure-Muret 1955; Malaroda et al. 1970). Our fieldwork has documented that Upper Carboniferous metasediments are cut at low angle by the Alpine cleavage, which is defined by tiny white mica and chlorite, and progressively grades to protomylonites and ultramylonites. Some outliers of Triassic rocks were involved within shear zones and strongly deformed (i) the Alpine cleavage defined by tiny phengitic micas is regionally observed (ii) upside down successions were recognized in the footwall of several reverse shear zones (iii) a plurihectometric recumbent south-verging fold involves the Triassic carbonates along the footwall of the E-W trending Tortisse reverse shear zone (Fig. 2).

5. Conditions of alpine deformation

Petrostructural observations allow to stress that any metamorphic or plutonic rock in the massif records at varying degrees the mechanical and thermal effects of Alpine reworking. Microscopic kink bands are ubiquitous in most biotites, even those from granites devoid of planar fabric. Cataclastic microstructures are also observed in quartz and K-feldspar from most granites, with crystallization of phengite. The nearly isotropic leucogranites of the eastern part of the massif are commonly brecciated. In these granites the network of fissures (from dm to mm scale) is sealed by minute streaky phengite along slickensides. Biotite in most rocks is partly replaced by small phengite crystals with numerous sagenite exsolutions, which suggest that the reaction K-feldspar + biotite + H_2O -> phengite + Fe chlorite + rutile took place. Other biotites may also show the development of a green biotite corona in equilibrium with phengitic micas.

Along the FSZ, the Argentera granite devoid of planar structure (sample MC8) grades into protomylonites (sample MC6b) in which the magmatic minerals are well preserved. Quartz shows undulose extinction with recrystallized matrix being less than 10-20 % vol. (Pl.1, Fig.a). Most of the magmatic biotite is recrystallized into phengite, green biotite and chlorite whereas scarce magmatic muscovite is only kinked.

In a more advanced stage of mylonitisation (sample MC7), the quartz porphyroclasts display a ribbon shape, K-Feldspars and plagioclases are truncated and the amount of phengites increases up to 20-30 % vol. (Pl.1, Fig.b). Preserved muscovite clasts are microfolded. Microcrystalline phengite is concentrated along small-scale shear bands cutting the feldspars. The core of the shear zone, up to 30m thick, consists of fine-grained mylonites to ultra-mylonites (sample MC6a). Microstructure of this rock shows the juxtaposition of distinct felsic bands enriched in quartz and thin (1-3 mm) layers with >80% phengitic micas formed as a consequence of complete breakdown of K-feldspars (Pl.1, Fig.c). The rare preserved muscovite fishes are totally surrounded and in part replaced by the phengitic matrix with small amounts of green biotite.

Protomylonites in the VSZ (MC24, 26 and 27) were derived from high-temperature two mica gneisses. Abundant pre-Alpine muscovites are preserved in the core of fishes and show a gradual recrystallisation towards their margin (Pl.1, Fig.d).

Pressure and temperature estimates during the Alpine deformation event are based on the coexistence of phengite and green biotite with Fe-rich compositions in felsic rocks and of the mineral assemblage clinozoisite, albite, actinote and chlorite observed regionally in retrogressed amphibolites and their crosscutting quartz veinlets. According to the petrogenetic grid of Powel & Holland (1990), the later paragenesis may indicate that regional temperatures at ca 350 °C were reached for pressure above 0.4 GPa. The Si content of phengite (3.20 – 3.29, Tab. 1) formed in both the K-rich granitoids and Early Triassic silty quartzites also constrains pressure around 0.35 – 0.4 GPa at this temperature (Massone 1995; Massonne & Schreyer 1987). Phengites in the Triassic rocks yield lower Si values (3.10 – 3.20) possibly due to the lack of detrital biotite in the initial material. Post-kinematic stilpnomelane has also been observed in some samples. These conditions are more severe than those recorded in the Pelvoux massif where no Alpine biotite has been observed (Aprahamian 1988; Seward et al. 1997) but are similar to those reported from the Mont Blanc and Aar Massifs (Marshall et al. 1998; Desmons et al. 1999).

6. ^{39}Ar-^{40}Ar results

Analytical Procedure

Single grains of muscovite and biotite used for the experiments were handpicked under a binocular microscope from the 0.25 to 0.8 mm fractions of the crushed rock samples. The samples were wrapped in Al foil to form small packets (11 x 11mm) that were staked up to form a pile within which packets of fluence monitors were inserted every 8 to 10 samples. The pile was irradiated for 70 hr at the McMaster reactor (Hamilton, Canada) with a total fluence of 9 x 10^{18} n.cm^{-2}. The irradiation standard was the amphibole Hb3gr (1072 Ma; Roddick, 1983).

Tab. 2. ^{40}Ar/^{39}Ar analytical data.

$^{40}Ar_{atm}$ = atmospheric ^{40}Ar. ^{40}Ar* = radiogenic ^{40}Ar. Ca = produced by Ca-neutron interferences. K = produced by K-neutron interferences. Age (Ma) = the date is calculated using the decay constants recommended by Steiger and Jäger (1977). The error are at the 1σ level and do not include the error in the value of the J parameter. Correction factors for interfering isotopes produced by neutron irradiation in the McMaster reactor were $(^{39}Ar/^{37}Ar)_{Ca} = 7.06x10^{-4}$, $(^{36}Ar/^{37}Ar)_{Ca} = 2.79x10^{-4}$, $(^{40}Ar/^{39}Ar)_K = 2.95x10^{-2}$.

Step n°	$^{40}Ar_{Atm}$ %	$^{39}Ar_K$ %	$^{37}Ar_{Ca}/^{39}Ar_K$	$^{40}Ar^*Ar_K$	Age (Ma)
MC24 Muscovite J=0.01781149					
1	33.1	0.7	1.50E-02	4.79	147.8 ± 6.0
2	4.4	2.2	1.20E-02	5.29	162.5 ± 2.1
3	14.6	2.0	3.00E-03	6.06	185.0 ± 2.1
4	2.5	2.4	5.00E-03	7.18	217.2 ± 2.8
5	0.7	4.3	3.00E-03	9.03	268.9 ± 1.2
6	0.5	34.2	1.00E-03	10.30	303.8 ± 0.5
7	0.5	5.5	5.00E-03	10.35	305.2 ± 1.0
8	0.8	3.8	6.00E-03	10.40	306.5 ± 1.4
9	0.4	13.3	1.20E-02	10.53	310.1 ± 0.6
10	0.0	4.7	3.00E-03	10.60	311.9 ± 1.3
fuse	0.1	27.0	0.00E+00	10.76	316.3 ± 0.7
				Integrated age:	298.8 ± 0.3
MC24 Biotite J=0.01782244					
1	36.9	0.3	6.00E-02	29.58	763.9 ± 15.0
2	7.8	6.7	9.00E-03	15.20	432.5 ± 1.4
3	3.6	6.7	4.00E-03	13.57	390.7 ± 1.1
4	1.8	7.1	3.00E-03	12.40	360.2 ± 1.1
5	2.9	8.6	5.00E-03	7.58	228.6 ± 0.9
6	1.4	6.1	4.00E-03	6.98	211.6 ± 1.1
7	1.4	6.0	4.00E-03	7.27	219.7 ± 1.2
8	1.3	5.3	5.00E-03	7.59	228.9 ± 1.2
9	0.4	14.4	3.00E-03	7.98	239.9 ± 0.5
10	0.4	14.5	2.00E-03	8.67	259.2 ± 0.5
11	0.8	5.5	2.00E-03	8.81	263.0 ± 0.9
12	1.2	4.2	2.00E-03	8.75	261.3 ± 1.6
13	1.1	6.1	2.00E-03	8.77	262.0 ± 1.3
14	0.6	5.2	2.00E-03	8.58	256.6 ± 1.3
fuse	1.0	3.3	1.00E-03	8.16	244.9 ± 2.0
				Integrated age:	277.2 ± 0.3
MC26 Muscovite J=0.01784478					
1	43.3	0.4	3.00E-03	3.32	104.0 ± 9.7
2	9.0	0.7	0.00E+00	4.27	132.5 ± 5.9
3	4.4	1.7	2.00E-03	5.93	181.6 ± 3.0
4	6.5	3.1	5.00E-03	7.58	228.8 ± 2.0
5	1.9	31.5	1.00E-03	10.18	301.1 ± 1.1
6	1.0	5.2	2.00E-03	9.48	282.1 ± 1.0
7	0.9	3.5	4.00E-03	10.03	297.1 ± 2.1
8	0.6	16.9	1.00E-03	10.58	311.9 ± 1.4
fuse	0.0	36.9	8.00E-03	10.73	316.2 ± 0.8
				Integrated age:	301.3 ± 0.5
MC26 Biotite J=0.01785577					
1	31.2	1.8	1.80E-02	8.25	248.0 ± 4.5
2	3.3	10.3	4.00E-03	10.79	317.9 ± 3.6
3	0.9	25.8	2.00E-03	10.39	307.1 ± 0.8
4	0.4	7.7	3.00E-03	9.85	292.2 ± 1.2
5	0.4	12.8	3.00E-03	9.63	286.4 ± 1.0
6	0.6	13.0	3.00E-03	9.74	289.4 ± 0.9
7	0.0	8.0	1.00E-03	10.13	300.0 ± 1.5
8	0.0	10.5	1.00E-03	10.53	310.8 ± 1.5
fuse	0.0	10.1	4.00E-03	10.52	310.6 ± 1.1
				Integrated age:	301.3 ± 0.5

Tab. 2 (continued)

Step n°	$^{40}Ar_{Atm}$ %	$^{39}Ar_K$ %	$^{37}Ar_{Ca}/^{39}Ar_K$	$^{40}Ar^*Ar_K$	Age (Ma)
MC27 Muscovite J=0.01786639					
1	20.6	1.3	5.00E-03	4.89	151.2 ± 4.0
2	4.6	2.5	4.00E-03	7.63	230.5 ± 1.8
3	1.7	6.9	2.00E-03	9.89	293.4 ± 1.2
4	0.6	18.4	1.00E-03	10.64	314.0 ± 1.1
5	0.5	11.9	1.00E-03	10.28	304.2 ± 0.9
6	0.9	5.8	1.00E-03	10.43	308.2 ± 1.6
7	0.4	12.3	0.00E+00	10.73	316.3 ± 0.8
8	0.2	7.4	0.00E+00	10.85	319.7 ± 0.9
fuse	0.0	33.5	0.00E+00	10.92	321.6 ± 0.7
					Integrated age: 310.3 ± 0.4
MC27 Biotite J=0.0178778					
1	100.0	0.3	1.50E-02	-0.03	0.0 ± 0.0
2	30.8	3.5	1.20E-02	1.40	44.6 ± 0.5
3	20.7	3.6	8.00E-03	4.16	129.5 ± 0.6
4	2.5	7.4	1.50E-02	6.30	192.6 ± 0.5
5	0.6	10.8	6.00E-03	6.53	199.2 ± 0.5
6	0.5	11.3	7.00E-03	7.00	212.8 ± 0.5
7	0.3	10.1	5.00E-03	7.44	225.3 ± 0.5
8	0.4	10.4	5.00E-03	7.56	228.6 ± 0.5
9	0.4	11.1	5.00E-03	7.33	222.2 ± 0.6
10	0.4	10.4	5.00E-03	7.15	217.0 ± 0.5
11	0.5	6.8	8.00E-03	7.65	231.3 ± 0.5
12	0.2	5.9	1.20E-02	8.95	267.7 ± 0.7
13	0.3	4.1	2.40E-02	9.26	276.5 ± 0.7
14	0.6	2.3	7.00E-03	9.27	276.5 ± 1.3
fuse	0.6	2.1	6.00E-03	8.32	250.3 ± 1.1
					Integrated age: 214.6 ± 0.2
MC6a Muscovite J=0.01799314					
1	2.0	8.1	3.00E-03	3.88	121.8 ± 3.0
2	0.0	29.8	0.00E+00	8.42	254.6 ± 1.6
3	0.2	7.9	1.00E-03	8.26	250.0 ± 3.3
4	0.3	33.4	2.00E-03	9.31	279.5 ± 1.0
5	0.6	10.9	3.00E-03	9.51	284.9 ± 2.0
fuse	0.0	9.8	2.00E-03	9.59	287.3 ± 2.7
					Integrated age: 258.8 ± 0.8
MC6a Phengite 1 J=0.01800511					
1	6.1	30.3	1.00E-03	0.64	20.6 ± 0.7
2	2.0	28.6	2.00E-03	0.68	22.1 ± 0.8
3	0.1	29.7	2.00E-03	0.70	22.6 ± 0.6
4	69.0	2.3	9.00E-03	0.21	6.7 ± 15.0
fuse	23.2	9.2	2.40E-02	0.54	17.5 ± 2.5
					Integrated age: 21.0 ± 0.5
MC6a Phengite 2 J=0.01800511					
1	0.0	7.6	6.00E-03	0.71	23.0 ± 2.3
2	0.0	13.2	1.00E-03	0.70	22.7 ± 1.5
3	0.4	27.4	2.00E-03	0.70	22.7 ± 0.6
4	3.6	34.1	2.00E-03	0.70	22.5 ± 0.4
fuse	7.7	17.7	3.00E-03	0.82	26.5 ± 0.6
					Integrated age: 23.3 ± 0.4

Tab. 2 (continued)

Step n°	$^{40}Ar_{Atm}$ %	$^{39}Ar_K$ %	$^{37}Ar_{Ca}/^{39}Ar_K$	$^{40}Ar^*Ar_K$	Age (Ma)
MC6a Phengite 3 J=0.01800511					
1	15.2	16.1	5.00E-03	0.60	19.4 ± 0.8
2	6.3	12.7	3.00E-03	0.65	21.0 ± 1.0
3	1.4	55.2	1.00E-03	0.69	22.4 ± 0.4
4	11.6	4.7	8.00E-03	0.63	20.5 ± 3.5
fuse	1.8	11.3	1.60E-02	0.71	23.0 ± 1.7
					Integrated age: 21.7 ± 0.4
MC6b Muscovite J=0.0180195					
1	63.5	0.3	8.00E-02	2.06	65.7 ± 123.8
2	12.8	4.4	8.00E-03	3.94	123.6 ± 12.5
3	0.6	50.7	0.00E+00	9.85	294.8 ± 1.6
4	1.1	38.3	1.00E-03	9.99	298.7 ± 1.7
fuse	2.4	6.4	3.30E-02	9.81	293.6 ± 7.9
					Integrated age: 288.4 ± 1.3
MC6b Green Biotite J=0.01803152					
1	76.9	0.7	1.11E-01	1.10	35.4 ± 22.5
2	68.5	2.7	07.20E-02	0.49	16.0 ± 5.4
3	40.7	5.7	6.50E-02	0.64	20.8 ± 2.6
4	8.4	7.1	5.50E-02	0.90	29.1 ± 2.0
5	6.3	10.8	4.50E-02	1.00	32.2 ± 0.9
6	4.1	15.9	3.40E-02	1.25	40.3 ± 0.8
7	7.4	20.4	3.30E-02	1.18	38.0 ± 0.5
8	5.5	12.5	5.20E-02	0.99	32.0 ± 0.9
9	4.3	6.1	1.56E-01	0.93	30.1 ± 1.5
10	7.8	18.2	1.27E+00	1.16	37.2 ± 0.7
					Integrated age: 34.1 ± 0.4
MC7 Muscovite J=0.01804354					
1	45.0	3.4	2.00E-03	2.04	65.1 ± 4.9
2	0.0	3.9	3.00E-03	3.24	102.3 ± 4.1
3	0.0	22.4	1.00E-03	8.43	255.5 ± 0.9
4	0.7	3.5	0.00E+00	8.67	262.1 ± 3.0
5	0.3	7.7	1.00E-03	9.38	282.1 ± 1.9
6	0.3	16.9	1.00E-03	10.00	299.2 ± 0.8
7	0.3	38.1	0.00E+00	10.12	302.6 ± 0.5
fuse	2.7	4.2	3.00E-03	9.58	287.7 ± 3.1
					Integrated age: 272.9 ± 0.4
MC8 Muscovite J=0.01805558					
1	22.8	0.5	0.00E+00	5.94	183.7 ± 9.4
2	1.4	3.0	0.00E+00	6.65	204.5 ± 2.4
3	0.2	1.9	0.00E+00	6.40	197.3 ± 3.6
4	0.4	38.1	1.00E-03	9.87	295.9 ± 0.4
5	0.4	37.7	1.00E-03	8.77	265.1 ± 0.7
fuse	0.2	18.8	1.00E-03	8.74	264.4 ± 0.7
					Integrated age: 273.3 ± 0.4
MC8 Biotite J=0.01806764					
1	8.8	1.5	1.30E-02	12.73	373.4 ± 2.2
2	2.3	15.1	9.00E-03	5.26	163.6 ± 0.4
3	0.8	28.0	8.00E-03	4.59	143.8 ± 0.2
4	0.3	42.8	1.90E-02	4.89	152.7 ± 0.2
5	0.4	6.2	9.50E-02	4.89	152.9 ± 0.9
6	9.4	3.3	3.99E-01	4.41	138.2 ± 1.4
fuse	0.3	3.1	5.65E-01	5.06	157.7 ± 1.3
					Integrated age: 155.2 ± 0.2

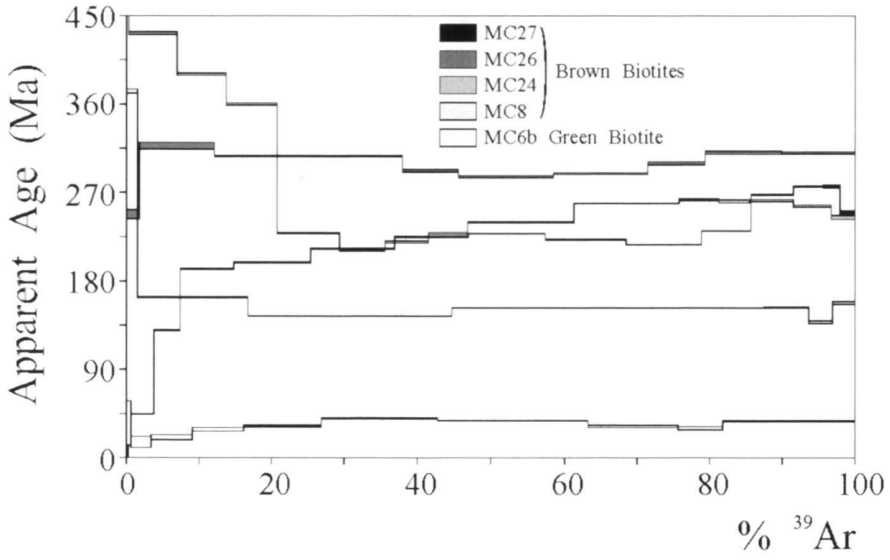

Fig. 3. $^{40}Ar/^{39}Ar$ age spectra (1σ relative uncertainties) of biotite samples. See Figure 2 for sample location and text for discussion.

The sample arrangement allows to monitor the flux gradient with a precision as good as ± 0.2%.

The step-heating experiment on single grains was described by Ruffet et al. (1991, 1995). Blanks are performed routinely each first or third step, and are subtracted from the subsequent sample gas fractions. Typical blank values were in the range $3.0 \times 10^{-13} <$ M/e40 $< 1.8 \times 10^{-12}$, $1.1 \times 10^{-14} <$ M/e39 $< 1.7 \times 10^{-13}$, $3.5 \times 10^{-16} <$ M/e38 $< 2.5 \times 10^{-14}$, $3.1 \times 10^{-14} <$ M/e37 $< 6.9 \times 10^{-14}$ and $3.9 \times 10^{-15} <$ M/e36 $< 1.5 \times 10^{-14}$ cm^{-3} STP. To define a plateau age, we need a minimum of three consecutive steps, corresponding to a minimum of 70% of the total $^{39}Ar_K$ released, and the individual fraction ages should agree within 2σ with the integrated age of the plateau segment.

^{39}Ar-^{40}Ar data

Five biotites and ten muscovite grains from twelve samples were analyzed with an argon-ion laser probe. Analytical data are displayed in table 2.

Biotites

The pre-Alpine biotites analyses provided disturbed age spectra with either saddle- or hump-shapes (Fig. 3). The oldest integrated ages, in the range 210-295 Ma, are displayed by samples collected in the Valetta Shear zone (MC24, 26 and 27). On the other hand, samples from the mylonitized Argentera granite within the FSZ (MC8 and MC6b) display younger integrated ages; the youngest one (33Ma) is displayed by a green biotite grain considered as newly grown Alpine phase (MC6b). The weakness of results displayed by pre-Alpine brown biotite samples, which are altered or partly recrystallized, does not allow to constrain the initial crystallization age nor the age of the subsequent disturbing event. Experiment performed on the Alpine green biotite of sample MC6b could display constraints on the age of this event. Nevertheless, the hump-shaped age spectrum yielded by this sample suggests, as earlier evidenced by e.g. Cheilletz et al. (1999), that the experiment is altered by a recoil of the ^{39}Ar as a consequence of the presence of chlorite interlayered in the biotite. In this topic the observed intermediate to high temperature apparent ages and integrated age are too old as a result of the displacement and probably loss of the neutron-induced atom during irradiation.

Muscovites

Three groups of results can be identified, according to the sampling context: the pre-Alpine muscovites from the migmatites within the Valetta shear zone (Fig. 4), the magmatic muscovites from the mylonitized Argentera granite within the FSZ (Fig. 5) and the Alpine phengites from the ultra-mylonitized Argentera granite, neocrystallized within the FSZ (Fig. 6).

The three analyzed muscovites from the Valetta shear zone (MC24, 26 and 27) display very similar staircase shaped age spectra (Fig. 4). The high temperature steps converge towards 305-315 Ma, as clearly shown by the frequency peak of apparent ages, whereas the low temperature increments display apparent ages between 104 Ma and 151 Ma. It was assumed for a long time that staircases in mica age spectra reflected diffusive argon loss but it is now accepted as proven by e.g. Wijbrans & McDougall (1986) or Villa (1998) that this is not the case. The high temperature apparent ages are minimal estimates the cooling or crystallization age of the mineral. Nevertheless, the weakly pronounced staircase shapes suggest that the high temperature apparent ages are close to the true age (cooling or crystallization age) of the mineral (305-315 Ma). A close look to the shape of the age spectra shows that two of them present a slight saddle shape in the intermediate temperature steps.

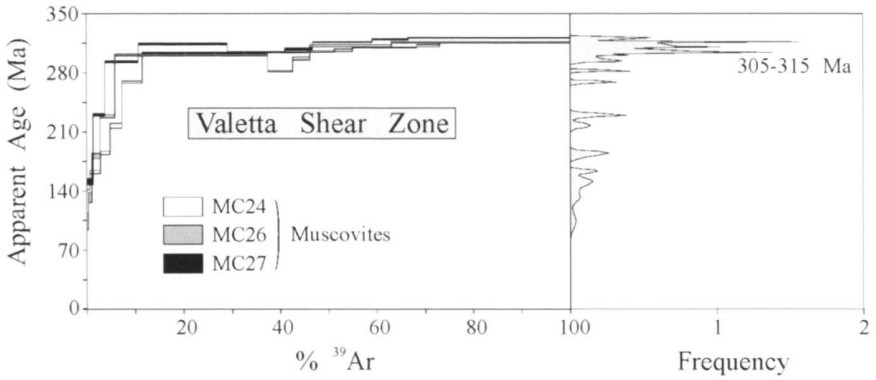

Fig. 4. $^{40}Ar/^{39}Ar$ age spectra (1σ relative uncertainties) of muscovite samples from migmatites deformed within the Valetta shear zone. See Figure 2 for sample location and text for discussion.

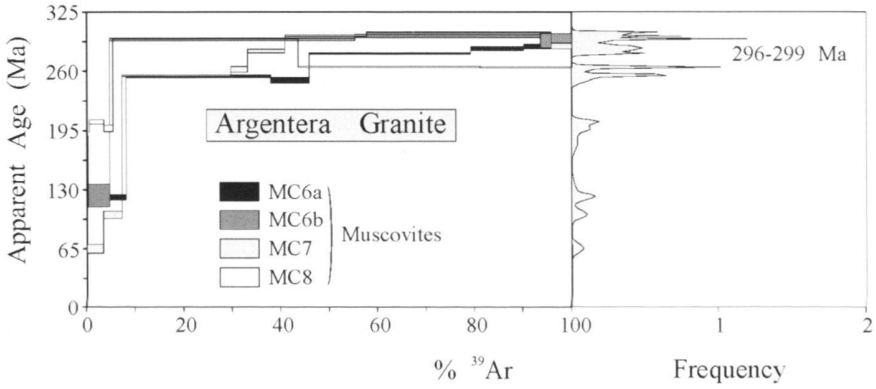

Fig. 5. $^{40}Ar/^{39}Ar$ age spectra (1σ relative uncertainties) of muscovites from Argentera granite deformed within the Frema Morte shear zone. See Figure 2 for sample location and text for discussion.

This feature can be indicative of some partial recrystallization of the muscovites into phengite which occurred during a disturbing event as shown by e.g. Cheilletz et al. (1999), Tremblay et al. (2000), Castonguay et al. (2001) or Alexandrov et al. (2002). Whatever it may be, the apparent low impact of the disturbing event on the K-Ar isotopic system of these samples does not allow to constrain precisely its age even if it is probably Alpine. We propose that these muscovites crystallized during the Hercynian high temperature metamorphism and were deformed and partly recrystallized during a shearing event of Alpine age.

Three muscovites from deformed samples (MC6a, MC6b and MC7) collected within the shear zone, which crosscuts the Argentera granite (FSZ) display age spectra (Fig. 5) with a shape similar to samples from the previous group. As discussed above, this shape may indicate that these samples also suffered a disturbing event but unfortunately it does not allow to further constrain its age. The convergence of the high temperature apparent ages and the apparently limited effect of the disturbance (shearing event) on their K-Ar isotopic system, shown by the weakly pronounced staircase shapes, suggest that these muscovites have an age around 296-299 Ma. This age probably characterizes cooling following the intrusion of the late orogenic Argentera granite. The less disturbed age spectrum is obtained on a protomylonitic sample MC6b. The less deformed sample (MC8) displays a very disturbed age spectrum, which remains hard to explain. Paradoxically, it seems more disturbed than muscovite from the ultramylonitic sample MC6a.

Three analyses were performed on phengites, which grew in the matrix of ultramylonite sample MC6a (Fig. 6). The size of the analyzed grains, which does not exceed 300 μm, can explain the slightly higher error bars. The three experiments display concordant age spectra, which allow to define an apparent age frequency peak at ca. 22.5 Ma. The mean age of the three calculated plateau ages is 22.2 ± 0.3 Ma. This age is interpreted as a crystallization age since the isotopic closure temperature of phengite is probably higher than the peak temperature reached during the regional metamorphism (e.g. Villa 1998).

7. Discussion and conclusion

Timing of Hercynian events

Rubatto et al. (2001) mentioned that one or two distinct HP-HT events could be identified in the Argentera Massif. At the moment, the age of this (these) HP-HT event(s) is poorly constrained. If there were two HP-HT events, the youngest one

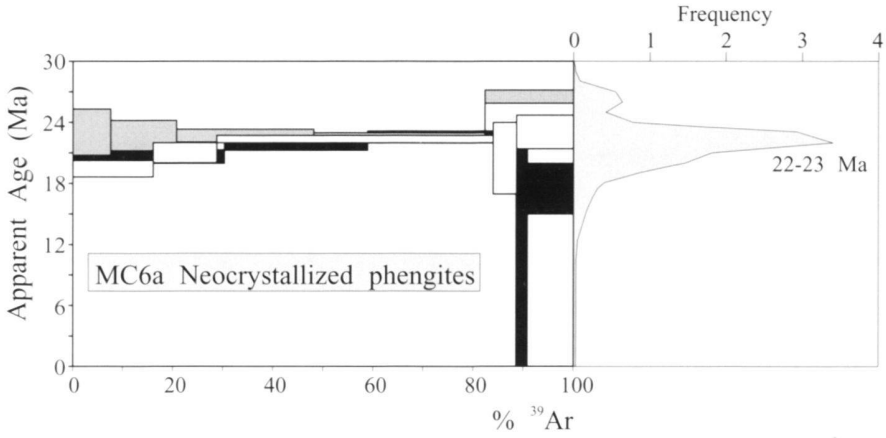

Fig. 6. $^{40}Ar/^{39}Ar$ age spectra (1σ relative uncertainties) of phengites neocrystallised within ultramylonites from the Frema Morte shear zone. See Figure 2 for sample location and text for discussion.

would be Devonian. In this case the old ^{39}Ar-^{40}Ar age on muscovite at 374 Ma obtained by Monié & Maluski (1983), on the assumption that it does not result from the presence of inherited argon, could be related to the early stage of metamorphism following HP-HT metamorphism (Latouche & Bogdanoff, 1987).

We interpret our ages around 310-315 Ma (samples MC 24, 26 and 27) measured on muscovites from the Valetta shear zone as cooling ages following a low pressure anatectic event, whose a maximum estimate is proposed at 323 ± 12 Ma by Rubatto et al. (2001), prior to late Hercynian (Stephanian) deformation stages. They also corroborate an ^{39}Ar-^{40}Ar biotite age at 315 ± 6 Ma obtained by Monié & Maluski (1983) for the Western Tinée complex.

A Rb-Sr study of the Argentera granite was performed by Ferrara & Malaroda (1969). The obtained age was recalculated (with $\lambda=1{,}42.10^{-11}an^{-1}$) by Monié & Maluski (1983) at 293 ± 10 Ma. It is in good agreement with our proposed age range at 296-299 Ma for the cooling of the granite but significantly older than the age at 275 ± 5 Ma proposed by Monié & Maluski (1983). Our data (296-299 Ma) allow to reject the hypothesis of the existence of a Permian migmatitic event ending around 275 Ma evocated by these authors and by Malaroda (1999) and references therein. We consider that the emplacement of the Argentera granite marks the end of the high temperature metamorphism and subsequent melting. According to Debon and Lemmet (1999), this late Variscan plutonic event, which took place during the Stephanian (between 295 and 305 Ma) is widespread in the External Crystalline massifs of the Western Alps. Therefore the Stephanian sediments might deposed during the 296-290 Ma interval.

Timing of the Alpine event

Monié & Maluski (1983) suggested that Hercynian minerals "remained closed until affected by the Alpine event at 40 Ma". This age was suggested on the basis of the mean of five discordant low temperature apparent ages displayed by a K-feldspar analysis. Recently, fission track thermochronology performed in the same area of the massif (Bigot-Cormier et al. 2000) confirmed that the early cooling of this domain and subsequently its uplift could occur in the time range 29-20 Ma according to zircon fission track. Our results at ca 22.5 Ma, from phengites, which have grown in an undoubted Alpine shear zone, noticeably rejuvenates the estimates of the Alpine age of deformation in the Argentera Massif. This age preclude that the mylonites cutting the Argentera granite may represent the superposition of Alpine overprint of late hercynian mylonites. It is the first unequivocal evidence of the existence of a late Alpine deformation and above all of metamorphism in the Argentera massif, and one of the first age constraints of the late Alpine history in the external massifs of the Western Alps.

Our P-T conditions estimates around 350°C and 0.35-0.4 GPa imply a minimum burial of 10-14 km for the Argentera massif, with a geothermal gradient of 25-35 $°C.km^{-1}$. This burial could result from the overloading imposed by the internal nappes emplacement during Alpine collision. In the foreland basin, to the southwest of the Argentera Massif, the emplacement of the Helminthoid flysch nappes occurred during the Chattian (28 Ma), which is the age of the youngest deposit prior to folding and thrusting in the foreland basin (Ford et al. 1999).

Our age at 22.5 Ma (Early Miocene) was obtained on synkinematic phengites grown in mylonites from a main ductile southward thrusting (FSZ) connected to a ductile dextral wrench fault (VSZ). The cooling of the Argentera Massif may have occurred just after this major Alpine compressive event that resulted in the shortening and southward displacement of the tectonic pile of sediments during the Early Miocene (Campredon & Giannerini 1982; Labaume et al. 1989; Guardia et al. 1996; Laurent et al. 2000).

In the same way, the maximum tectonic burial of the Pelvoux External Crystalline Massif is related to the overloading of the internal nappes, as can be observed at its southern part where the Briançonnais, Sub-Briançonnais and Helminthoid flysch nappes are also part of the tectonic pile.

This can be also observed in the flexural foreland basin of Champsaur sandstones (Meckel et al. 1996; Seward et al., 1997). Furthermore the exhumation and the cooling of the Pelvoux Massif attributed to thrusting took place between 20 and 15 Ma (Fügenscuh & Schmid 2003). This stage is concomitant to the Internal Zone sin-collision normal faulting suggesting apparent extension, which started during Late Oligocene-Early Miocene (between 28 and 21 Ma) and is still active (Tricard et al. 2001). In the Mont Blanc Massif, fission tracks analyses on zircons from the Mont Blanc granite (11-13 Ma, Seward and Mancktelow 1994) and ^{39}Ar-^{40}Ar analyses on white micas from its sedimentary cover (27 to 15 Ma, Diableret unit, Crespo-Blanc et al. 1995; 19 to 17 Ma, Morcles unit, Kirchner et al. 1995) seems to confirm the Miocene age of the major phase of shortening coeval with greenschist facies metamorphism in most of the External Crystalline Massif of the Western Alps.

REFERENCES

ALEXANDROV, P., RUFFET, G., CHEILLETZ, A. 2002: Muscovite recrystallization and saddle-shaped $^{40}Ar/^{39}Ar$ age spectra: example from the Blond granite (French Massif Central). Geochim. et Cosmochim. Acta 66, 10, 1793–1807.

APRAHAMIAN, J.1988: Cartographie du métamorphisme faible à très faible dans les Alpes françaises externes par l'utilisation de la cristallinité de l'illite. Geodinam. Acta 2, 25–32.

BIGOT-CORMIER, F., POUPEAU, G., SOSSON, M. 2000: Dénudations différentielles du massif cristallin externe alpin de l'Argentera (Sud-est de la France) révélées par thermochronologie traces de fission (apatites, zircons). C. R. Acad. Sci. (Paris) 330, 363–370.

BOGDANOFF, S. 1980:Analyse structurale dans la partie occidentale de l'Argentera-Mercantour (Alpes–Maritimes). Thèse d'Etat, Univ. Orsay.

BOGDANOFF, S., MÉNOT, R. -P., VIVIER, G. 1991: Les massifs cristallins externes des Alpes occidentales françaises, un fragment de la zone interne varisque. Sci. géol. Bull. 44, 237–285.

BOGDANOFF, S., MICHARD, A., MANSOUR, M., POUPEAU, G., 2000: Apatite fission track analysis in the Argentera massif: evidence of contrasting denudation rates in the External Crystalline massifs of the Western Alps. Terra Nova 12, 3, 117–125

CAMPREDON, R. 1977: Les formations paléogènes des Alpes Maritimes franco-italiennes. Mém. Soc. Géol. France 9, 197 pp.

CAMPREDON, R., GIANNERINI, G.1982: le synclinal de Saint Antonin (arc de Castellane, chaînes subalpines méridionales). Un exemple de bassin soumis à une déformation compressive permanente depuis l'Eocène supérieur. Géologie Alpine 58, 15–20.

CASTONGUAY, S., RUFFET, G., TREMBLAY, A., FÉRAUD G. 2001: Tectonometamorphic evolution of the southern Quebec Appalachians: $^{40}Ar/^{39}Ar$ evidence for Ordovician crustal thickening and Silurian exhumation of the internal Humber zone. Geol. Soc. Amer. Bull. 113, 1, 144–160.

CHEILLETZ, A., RUFFET, G., MARIGNAC, C., KOLLI, O., GASQUET, D., FÉRAUD, G. AND BOUILLIN J.P. 1999: $^{40}Ar/^{39}Ar$ dating of shear zones in the Variscan basement of Greater Kabilia (Algeria). Evidence of an Eo-Alpine event at 128 Ma (Hauterivian-Barremian boundary): geodynamic consequences. Tectonophysics 306, 97–116.

CRESPO-BLANC, A., MASSON, H., SHARP, Z., COSCA M., HUNZIKER, J. 1995: A stable and 40Ar/39Ar isotope study of a major thrust in the Helvetic nappes (Swiss Alps): evidence for fluid flow and constraints on nappe kinematics. Geol. Soc. Amer. Bull. 107, 1129–1144.

DEBON, F., LEMMET, M. 1999: Evolution of Mg/Fe ratios in late variscan plutonic rocks from the external crystalline massifs of the Alps (France, Italy, Switzerland). J. Petrol. 40, 1151–1185.

DESMONS, J., APRAHAMIAN, J., COMPAGONI, R., CORTESOGNO, L., FREY. M. 1999: Alpine metamorphism of the Western Alps. Middle to high T/P metamorphism. Schweiz. Miner. Petrogr. Mitt. 79, 89–110.

FAURE-MURET, A. 1955: Études géologiques sur le massif de l'Argentera-Mercantour et ses enveloppes sédimentaires. Mém. Soc. Géol. France. 336 pp.

FERRARA, G., MALARODA, M. 1969: Radiometric age of granitic rocks from the Argentera massif (Maritime Alps). Boll. Soc. Geol. It. 88, 311–320.

FORD, M. 1996: Kinematics and geometry of early Alpine, basement-involved folds, SW Pelvoux Massif, SE France. Eclogae Geol. Helv. 89, 269–295.

FÜGENSCHUH, B., SCHMID, S. M. 2003: Late stages of deformation and exhumation of an orogen constrained by fission-track data: A case study in the Western Alps. GSA Bulletin 115, p.

FORD, M., LICKORISH, W. H., KUSZNIR 1999: tertiary foreland sedimentation in the Southern Subalpine Chains, SE France: a geodynamic appraisal. Basin research 11, 315–336.

GOURLAY, P. 1986: La déformation du socle et des couvertures delphino-helvétiques dans la région du Mont-Blanc (Alpes occidentales). Bull. Soc. Géol. France (8) 1, 159–169.

GUARDIA, P., IVALDI, J. -P., DUBAR M., GUGLIELMI, Y., PEREZ, J. -L. 1996: Paléotectonique linéamentaire et tectonique active des Alpes maritimes franco-italiennes: une synthèse. Géol. France 1, 43–55.

KERCKHOVE, C. 1969: La "zone du Flysch" dans les nappes de l'Embrunais-Ubaye (Alpes occidentales). Géologie Alpine 45, 204 pp.

KIRSCHNER, D. L., SHARP, Z. D., MASSON, H. 1995: Oxygen isotope thermometry of quartz-calcite veins: Unraveling the thermal-tectonic history of the subgreenschist facies Morcles nappe (Swiss Alps). Geol. Soc. Amer. Bull. 107, 1145–1156.

LABAUME, P., RITZ, J.-F., PHILIP, H. 1989: Failles normales dans les Alpes sud-occidentales: leur relation avec la tectonique compressive. C. R. Acad. Sci. (Paris) 308, 1553–1560.

LATOUCHE, L., BOGDANNOFF, S. 1987: Évolution précoce du massif de l'Argentera: apport des éclogites et des granulites. Géologie alpine 63, 151–164.

LAURENT, O., STEPHAN, J.-F., POPOFF, M. 2000: Modalités de la structuration miocène de la branche sud de l'arc de Castellane (chaînes subalpines méridionales). Géol. France 3, 33–65.

MCDOUGALL, I., HARRISON, T.M. 1999: Geochronology and thermochronology by the $Ar^{4O} - Ar^{39}$ method. Oxford Monograph on Geology and Geophysics, Oxford Univ. Press 9, New York, 212p.

MALARODA, R., CARRARO, F., DAL PIAZ, G.V., FRANCESCHETTI, B., STURANI, C, ZANELLA, E. 1970: Carta geologica del Massicio dell'Argentera alla scala 1:50.000 e Note illustrative. Mem. Soc. Geol. A. IX, 557–663.

MALARODA, R. 1999: L'Argentera meridionale. Memoria illustrativa della "Geological Map of Southern Argentera Massif (Maritime Alps) 1: 25 000". Mem. Sci. Geol. Padova 51, 241–331.

MARQUER, D. 1990: Structures et déformation alpine dans les granites hercyniens du massif du Gothard (Alpes centrales suisses). Eclog. Geol. Helv. 83, 77–97.

MARSHALL, D., PFEIFER, H.-R., HUNZIKER, J. C., KIRSCHNER, D. 1988: A pressure-temperature-time path for the NE Mont-Blanc massif: Fluid-inclusion, isotopic and thermobarometric evidence. Eur. J. Mineral. 10, 1227–1240.

MASSONE, H. J., SCHREYER, W. 1987: Phengite barometry based on the limiting assemblage with K-feldspar, phlogopite and quartz. Contr. Miner. Petrol. 96, 212–214.

MASSONE, H. J. 1995: Experimental and petrogenetic study of UHPM. In: Ultrahigh pressure metamorphism, Eds. COLEMAN, R. G., WANG, X., Cambridge University press, 35–95.

MECKEL, L. D., FORD, M., BERNOUILLI, D. 1996: Tectonic and sedimentary evolution of the Devoluy Basin, a remnant of the Tertiary western Alpine foreland basin, SE France, Géol. France 2, 3–26.

MONIÉ, P., MALUSKI, H. 1983: Données géochronologiques Ar^{39}–Ar^{4O} sur le socle anté-Permien du massif de l'Argentera-Mercantour (Alpes-Maritimes, France). Bull. Soc. Géol. France 7, 247–257.

MUGNIER, J.-L, GUELLEC, S., MÉNARD, G., ROURE, F., TARDY, M., VIALON, P. 1990: A crustal scale balanced cross-section through the external Alps deduced from the ECORS profile. Mém. Soc. Géol., 156, 203–216.

PAQUETTE, J.-L., MÉNOT, R.P., PEUCAT, J.J. 1989: REE, Sm-Nd and U-Pb zircon study of eclogites from the Alpine external massifs (Western Alps): evidence for crustal contamination. Earth Planet. Sci. Lett. 96, 181–189.

POWELL, R., HOLLAND, T. 1990: Calculated mineral equilibria in the pelite system, KFMASH (K2O-FeO-MgO-Al2O3-SiO2-H2O). Am. Miner. 75, 367–380.

RODDICK, J. C. 1983: High precision intercalibration of $^{40}Ar/^{39}Ar$ standards: Geochim. Cosmochim. Acta 47, p. 887–898.

RUBATTO, D., SCHALTEGGER, U., LOMBARDO, B., COLOMBO, F., COMPAGNONI, R. 2001: Complex Paleozoic magmatic and metamorphic evolution in the Argentera Massif (Western Alps) resolved with U–Pb dating, Schweiz. Minéral. Petrogr. 81, 213–228.

RUFFET, G., FÉRAUD, G., AND AMOURIC, M. 1991: Comparison of $^{40}Ar/^{39}Ar$ conventional and laser dating of biotites from the North Trégor Batholith. Geochim. Cosmochim. Acta 55, 1675–1688.

RUFFET, G., FÉRAUD, G., BALLÈVRE, M., KIÉNAST, J. -R. 1995: Plateau ages and excess argon on phengites: a ^{40}Ar-^{39}Ar laser probe study of Alpine micas (Sesia zone). Chemical Geology, 121, 327–343.

SEWARD, D., FORD, M., BÜRGISSER, J., LICKORISH, H., WILLIAMS, E. A., MECKELII, L. D. 1997: Preliminary results of fission-track analyses in the Southern Pelvoux area, SE France. 3rd Workshop on Alpine Geological Studies, Oropa-Biella (Italia). Mem. Sci. Geol., 25–31.

SEWARD, D., MANCKTELOW, N. S. 1994: Neogene kinematics of the central and western Alps: Evidence from fission-track dating. Geology 22, 803–806.

STEIGER R.H., JÄGER E. 1977: Subcommission on geochronology: convention on the use of decay constants in geo- and cosmochronology. Earth Planet. Sci. Lett. 36, 359–362.

TREMBLAY A., RUFFET G. AND CASTONGUAY S. 2000: $^{40}Ar/^{39}Ar$ data bearing on plutonism and regional metamorphism in the Dunnage zone of southern Quebec, northern Appalachians. Geol. Soc. Amer. Bull. 112, 1, 136–146.

TRICART, P., SCHWARTZ, S., SUE, C., POUPEAU, G., LARDEAUX, J.-L. 2001: La dénudation tectonique de la zone ultradauphinoise et l'inversion du front briançonnais au sud-est du Pelvoux (Alpes occidentales): une dynamique miocène à actuelle. Bull. Soc. Géol. France 172, 49–58.

VERNET, J. 1964: La zone "Pelvoux-Argentera". Étude sur la tectonique alpine du socle dans la zone des massifs cristallins externes du Sud des Alpes occidentales. Thesis, Univ. Grenoble.

VILLA, I. M. 1998: Isotopic closure: Terra Nova 10, p. 42–47.

VON RAUMER, J. F., NEUBAUER, F. 1993: Pre-Mesozoic geology in the Alps. Ed. Springer-Verlag. 677 pp.

WIJBRANS, J.R. AND MCDOUGALL, I. 1986. $^{40}Ar/^{39}Ar$ dating of white micas from an alpine high-pressure metamorphic belt on Naxos (Greece): the resetting of the argon isotopic system. Contrib. Mineral. Petrol., 93, 187–194.

Manuscript received December 19, 2002
Revision accepted November 10, 2003

Plate 1: Optical photo micrographs of samples with crossed polars.
Sample MC6b: protomylonite of granite in which the magmatic minerals are preserved showing elongated quartz porphyroclasts.
Sample MC7: mylonite of granite showing truncated feldspar porphyroclasts and fine-grained quartz, feldspar and phengite recrystallized matrix.
Sample MC6a: ultramylonite of granite showing tabular quartz porphyroclasts with undulose extinction, thin bands of feldspar and quartz alternated with abundant phengitic matrix.
Sample MC24: mylonite of gneisses showing muscovite porphyroclast with undulose kink-band.
Note the increase of fine-grained recrystallized phengitic matrix from (a) to (c).
bi = biotite; fd = feldspar; qtz = quartz; mu = muscovite; ph = phengite.
Scale bar is 1 mm.

fd
mu
qtz
bi
a
ph
fd
b
qtz
ph
c
mu
ph
d